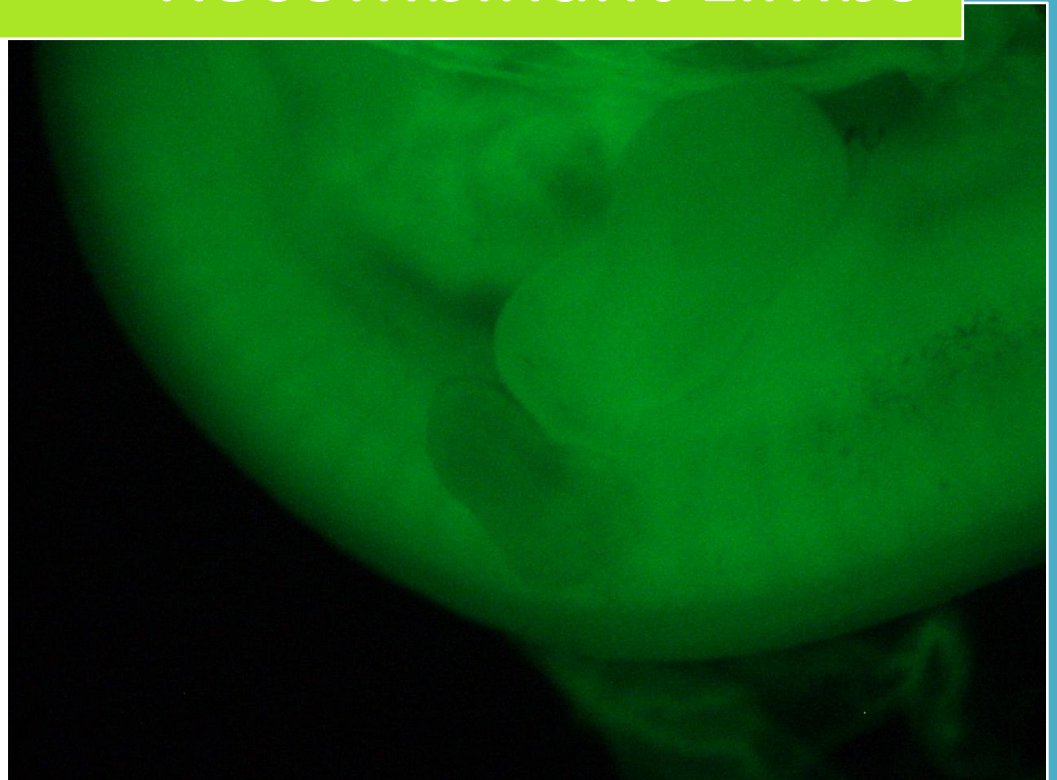


2012-2013

Proximo-Distal Sorting-out of Mesenchymal Cells in Recombinant Limbs



Master en Biomedicina y Biología Molecular

UC-UPV/EHU. IBBTEC (CSIC-UC-SODERCAN)

Santander.Cantabria

Autor: SARA LUCAS TOCA

Director: MARIAN ROS

INDEX

ABBREVIATIONS.....	3
INTRODUCTION.....	4
1. Brief introduction to the development of the vertebrate limb.....	4
2. Patterning along the proximo-distal axis.....	6
3. The experimental model of Recombinant Limbs.....	10
4. GFP-transgenic chicken.....	12
AIM OF THIS WORK.....	13
MATERIALS AND METHODS.....	14
1. Chicken embryos.....	14
2. Procedure to perform recombinant limbs.....	14
3. Paraffin embedding.....	16
4. Whole mount <i>in situ</i> hybridization	17
5. <i>In situ</i> hybridization in paraffin sections	17
RESULTS.....	18
1. Cells with different proximo-distal origin sorting out in the Recombinant Limb situation and localize according to their origin	18
2. The distribution of cells correlates with their Proximo-distal origin.....	22
3. The expression of <i>Gfp</i> is not the cause of the sorting out between proximal and distal cells.....	26
DISCUSSION.....	27
FUTURE EXPERIMENTS.....	29
CONCLUSIONS.....	30
ACKNOWLEDGEMENTS.....	31
REFERENCES.....	32

ABBREVIATIONS

AER Apical Ectodermal Ridge

AP Antero-Posterior

BMP Bone Morphogenetic Protein

DV Dorso-Ventral

ESM Early Specification Model

FGF Fibroblast Growth Factor

h Hours

HH Hamburger and Hamilton

ON Over night

PBS Phosphate Buffered Saline

PD Proximo-Distal

PFA Paraformaldehyde

PZ Progress Zone

PZM Progress Zone Model

RA Retinoic Acid

RT Room Temperature

Shh Sonic hedgehog

WT Wild type

ZPA Zone of Polarizing Activity

ISH *In situ* Hybridization

INTRODUCTION

1. Brief introduction to the development of the vertebrate limb

Embryonic development requires a careful control of proliferation, cell differentiation, patterning and cell death among other processes. The development of the vertebrate limb is one of the premiere systems to study pattern formation and morphogenesis. Decades of extensive study in two principal models, the chick and the mouse, have generated a considerable amount of very valuable information.

The early limb buds emerge from the lateral body wall as swellings of rapidly-dividing cells derived from lateral plate mesoderm. Limb buds are formed by an external ectodermal hull and a core of mesoderm. The interactions between the ectoderm and mesoderm components (ectodermal-mesenchymal interactions) are crucial for the further development of the limb bud.

Developing vertebrate limbs display three obvious axes of asymmetry: the proximo-distal (PD; shoulder to fingers), the anterior-posterior (AP; thumb to little finger) and the dorso-ventral (DV; from back of hand to palm). As the limb bud emerges, three distinct signaling centers that direct proper outgrowth and patterning in each axis, are established: the apical ectodermal ridge (AER), the zone of polarizing activity (ZPA) and the non-AER ectoderm.

Growth and patterning in the PD axis is controlled by the AER mainly through the secretion of a battery of fibroblast growth factors (Fgfs) (Mariani et al., 2008) (**Fig.1A**). During limb development the skeletal elements are specified in a proximo-distal manner progressive forming the stylopod (upper limb), then the zeugopod (lowerlimb) and finally the autopod (hand/foot) (**Fig.1D**). *Meis1/2*, *Hoxa11* and *Hoxa13* are considered the best markers of the stylopod, zeugopod and autopod respectively, although none of them are sufficient to specify limb-segment identity. (Tabin and Wolpert, 2007)

The ZPA is a group of posterior mesenchymal cells that controls AP patterning through the production of the potent signaling molecule Sonic Hedgehog (Shh) (Tickle et al., 1985; Ridle et al., 1993) (**Fig.1B**). AP patterning determines the number and the identity of the digits (Bastida et al., 2009).

Finally, DV patterning is controlled by the non-AER ectoderm. *Wnt7a* is expressed in the dorsal ectoderm (**Fig.1C**) (Altabef and Tickle, 2002; Dealy et al., 1993; Parr and McMahon, 1995; Parr et al., 1993) and some members of the Bone morphogenetic protein (Bmp) family (*Bmp2* and *Bmp4*) in the ventral ectoderm (Ahn et al., 2001; Pizette et al., 2001). *Wnt7a* induces the expression of the

transcription factor *Lmx1b* in the dorsal mesoderm (Riddle et al., 1995; Vogel et al., 1995) which will determine the dorsal identity of the mesoderm (Rodriguez-Esteban et al., 1997). In the ventral ectoderm BMP signaling, through BMPR1a, activates *En1* (Ahn et al., 2001; Pizette et al., 2001) that in turn restricts *Wnt7a* expression to the dorsal ectoderm thus conferring ventral identity (Davis et al., 1991; Gardner and Barald, 1992).

These three signaling systems are interconnected to assure the acquisition of the correct limb morphology and growth. Integration of three-dimensional patterning implies complex crosstalk among the Fgf, Shh, Wnt and Bmp signaling pathways (Bastida et al., 2009).

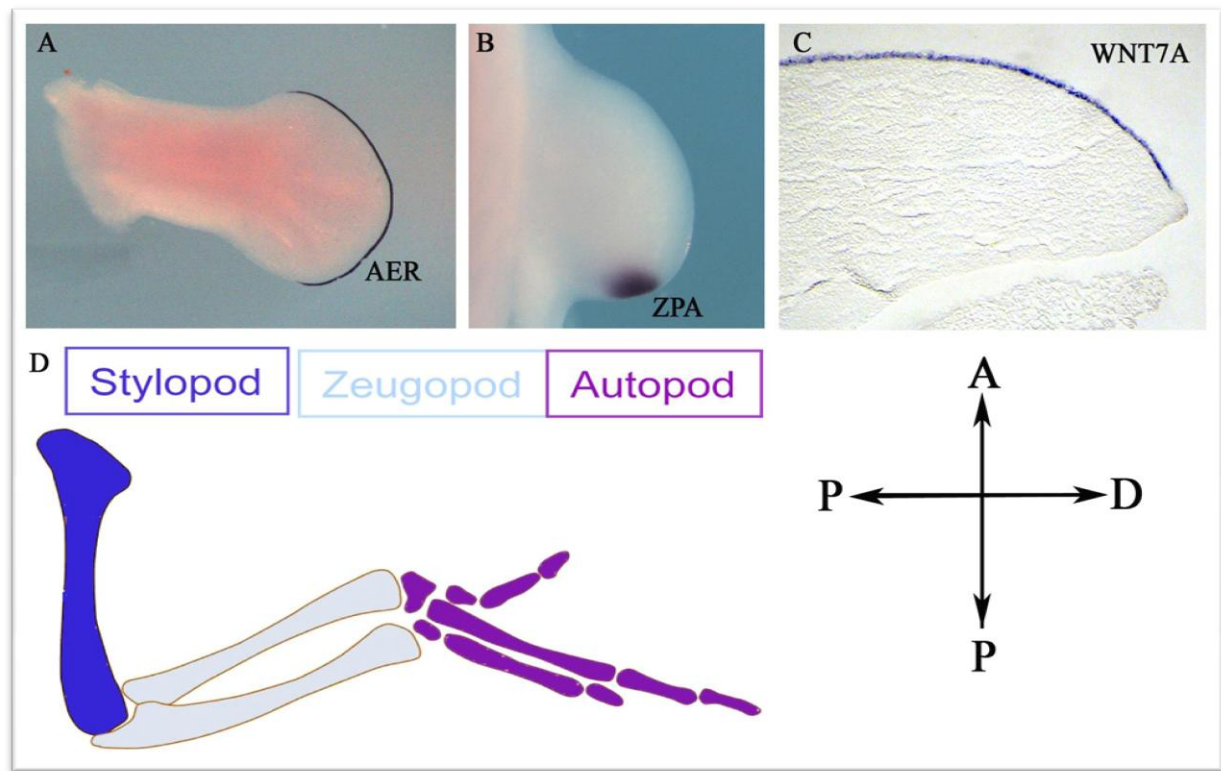


Figure 1: (A) Whole mount *in situ* hybridization showing *Fgf8* expression in the AER (B) *Shh* expression in the ZPA (C) and *in situ* hybridization in paraffin sections showing *Wnt7a* in the dorsal ectoderm. (D) Diagram showing the PD skeletal pattern of the mature chick limb in which the stylopod, the zeugopod and the autopod are marked.

In particular, the interaction between the ZPA and the AER is crucial for the correct growth and patterning of the limb. There is a positive feed-back loop between the Shh and the Fgf signaling pathways: Fgf from the AER is necessary for *Shh* expression in the ZPA and in turn Shh is necessary for maintenance of *Fgf* expression in the AER (Laufer et al., 1994; Niswander et al., 1994). *Grem1* an antagonist of Bmps, is the key intermediate in this interaction. Initially, Bmp signaling activates

Grem1 starting the limb developmental program. On the other hand, once the ZPA is established, *Shh* induces *Grem1* expression (Benazet et al., 2009; Nissim et al., 2006) (**Fig.2A**) and *Grem1* in turn antagonizes BMP-mediated inhibition of *Fgf* expression in the AER (Khokha et al., 2003; Michos et al., 2004). In a final step of the loop, *Fgfs* from the AER maintain *Shh* expression in the ZPA (**Fig.2B**).

Finally, two theories have been proposed for termination of the *Shh*-*Gremlin*-*Fgf* feed-back loop, once is that high FGF activity from the AER inhibits *Grem1* terminating this feed-back loop (Verheyden and Sun 2008) (**Fig.2C**). The other theory is that since *Shh*-expressing cells and their descendants cannot express *Gremlin*, the proliferation of these descendants forms a barrier separating the *Shh* signals from *Gremlin*-expressing cells, which breaks down the *Shh*-*Gremlin*-*Fgf* feed-back loop (Scherz et al., 2004). Recently research shows evidences that *Tbx2* directly represses *Grem1* in distal regions of the prosterior limb mesenchyme allowing *Bmp* signaling to abrogate *Fgf* expression in the AER (Farin et al., 2013)

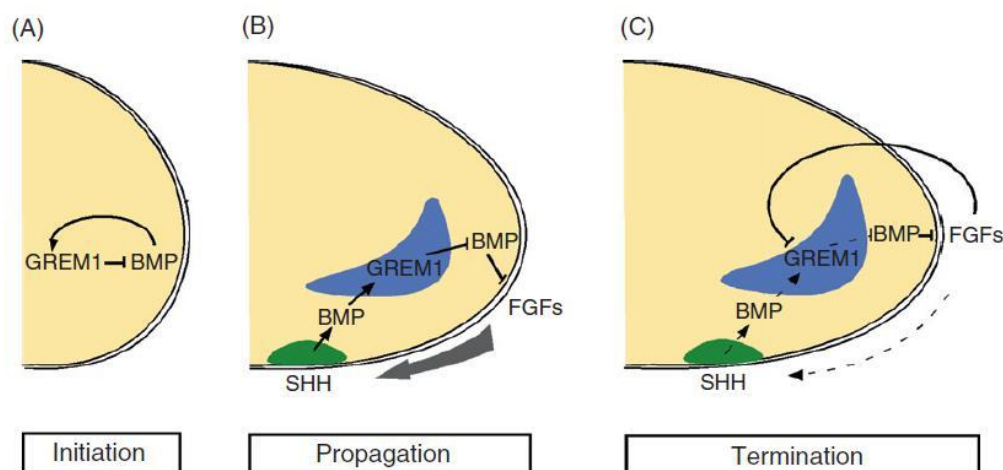


Figure 2: Interaction between the ZPA and the AER. (A) In the early limb bud BMP signaling induces *Grem1*. (B) Once *Shh* is activated, the *Shh*-*Grem1*-*Fgf* loop is established. (C) High levels of AER-*Fgfs* block *Grem1* expression thus resulting in an increase in BMP action that blocks *Fgf* signaling leading to the termination of the feed-back loop (From *Vertebrate Limb Patterning*, Natalie C. Butterfield et al., 2010).

2. Patterning along the proximo-distal axis

Pattern formation can be considered as a two-step process; first cells are informed of their position and, thus, acquire a positional value (specification); cells then remember and interpret this value to form the appropriate structures (differentiation) (Wolpert, 1969). The chick and the mouse skeleton have the typical vertebrate plan with three main regions along the PD axis, humerus, radius/ulna and digits together with a variable number of wrist elements (**Fig. 1D**).

Although it is not completely known how PD patterning is established and the mechanism that controls it, it is assumed that *Hox* genes, *Meis 1/2*, retinoic acid (RA) and *Fgfs* are implicated in this process. The paralogs of the 5'end of the *HoxA* and *HoxD* clusters are expressed in specific domains in the limb bud (Duboule, 1994; Duboule and Morata, 1994; Tabin, 1991; Zakany and Duboule, 1999). *Hoxa9-13* are expressed along the PD axis in specific patterns, being *Hoxa13* the most distal one. According to expression patterns and genetic ablations of these genes (Davis et al., 1995; Fromental-Ramain et al., 1996; Kondo and Duboule, 1999) it was proposed (Davis et al., 1995) that Hox genes would specify each segment of the limb; group 9-10 would specify the stylopod, group 11 the zeugopod and groups 12-13 the autopod.

Several models have been proposed over the years to explain PD patterning. In 1973 Wolpert and colleagues proposed the **Progress Zone Model (PZM)** (Summerbell et al., 1973). Removal of the AER at different stages of wing development causes truncations that progressively become more distally restricted the later the operations were performed. To explain these and others experiments, it was proposed that the length of time that undifferentiated mesenchymal cells spend proliferating at the tip of the limb – in a region known as the Progress Zone (PZ)– specifies PD positional values.

According to this model cells in the PZ are continuously proliferating and undifferentiated and they don't fix their fate until they leave this zone. Once they leave the PZ, they would differentiate according to the time they spent in the PZ. The more time the cells spend in the PZ the more distal structures they will form (**Fig.3**). The PZM requires a mechanism by which the cells would count the time spent in the PZ. It was proposed that it could be the number of cell divisions. Specification of PD pattern depends on growth, timing and length of exposure of a population of undifferentiated mesenchyme cells to a permissive AER signal.

The PZM satisfactorily explained all the phenotypic outcomes from experimental and genetic manipulations until the phenotypes of the genetic inactivation of *Fgf4* and *Fgf8* in the AER were obtained (Sun et al., 2002).

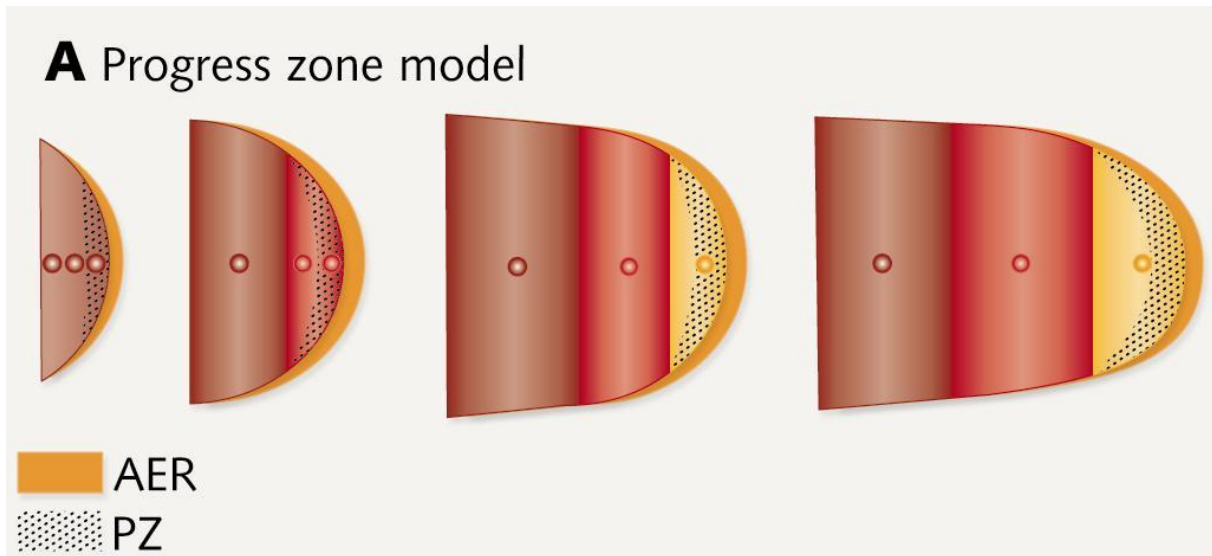


Figure 3: Diagrams representing the Progress Zone Model.

Brown, red and yellow indicate stylopod, zeugopod and autopod respectively.

Concomitantly, the **Early Specification Model (ESM)** (Dudley et al., 2002) was then proposed to give an explanation to the new phenotypes obtained. This model posits that the three PD elements are already specified from very early stages and they just sequentially elongate as the limb bud grows (**Fig.4**). The ESM explains the AER removal experiments based on the cell death produced after its removal in the distal mesoderm (Rowe et al., 1982; Dudley et al., 2002). This constant domain of cell death could explain the loss of the distal elements. Over time, the domain of cells affected contains a progressively smaller proportion of distal limb skeletal progenitor and this would explain why the truncation is more distal when the AER is removed at later stages. The absence of identified candidate genes to specify the three limb segments rests support to this model.

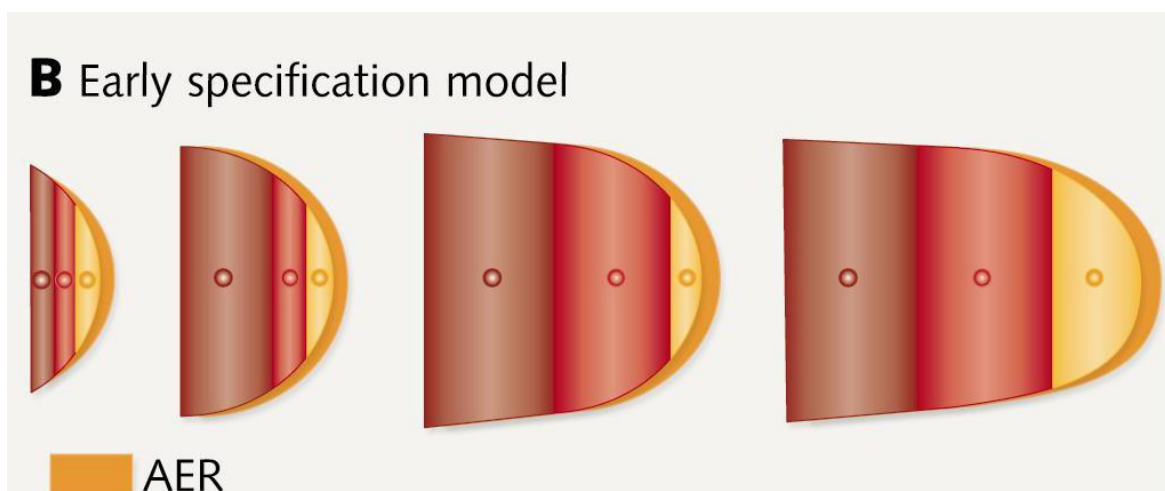


Figure 4: Diagrams representing the Early Specification Model.

(Same color code as in Fig. 3).

Based on the phenotypes of the limb-conditional knock-out (KO) mice for *Fgf8*, *Fgf4* and *Fgf9* in 2008 Gail Martin and colleagues proposed the two-signal model (Mariani et al., 2008). The two-signal model proposes that limb bud cells are initially exposed to a proximal signal from the flank mesoderm, possibly retinoic acid, and then to an opposing distal signal (Fgf) from the AER, which establishes proximal and distal domains, respectively (Mercader et al., 2000; Tabin and Wolpert, 2007). Formation of a third (middle) domain might then occur as a result of interactions between cells at the boundary between proximal and distal domains over time, thus creating the three domains from which the stylopod, zeugopod and autopod segments will develop.

Finally, a new model also called the **Two-signal Model** has been proposed by the group of Miguel Torres (Rossello-Diez et al., 2011) (**Fig.5**). This model differs from the previously proposed by Gail Martin and proposes that limb bud cells are initially exposed to two opposing signals one proximal signal from the flank mesoderm, possibly RA, and a second distal signal from the AER (Fgf signaling). As the limb bud grows, the cells in the distal limb bud lie out of the influence of the proximal signal, and as a consequence two domains, one proximal that would become the stylopod and one distal, are specified. The distal domain will later, in a second phase, be subdivided into the intermediate zeugopod and the distal autopod. It should be noted that although RA has been proposed as the proximal signal, this is a topic of huge controversy at present with recent reports indicating that RA signaling is not required for limb bud outgrowth or patterning (Zhao et al., 2009, Cunningham et al., 2013).

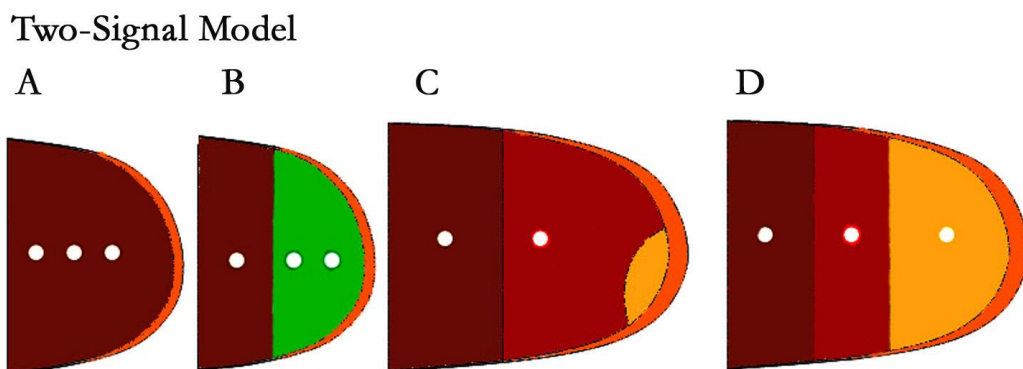


Figure 5: Diagram representing the Two-Signal Model. Brown, red and yellow indicate stylopod, zeugopod and autopod respectively. Green indicates the undifferentiated distal area and orange indicates the AER.

3. The experimental model of Recombinant Limbs

A recombinant limb (RL) can be briefly described as a limb-like structure created by experimentally assembling limb bud mesoderm inside a limb bud ectodermal jacket. When grafted to an appropriate site of a host embryo (e.g. somites or dorsal limb bud), the RLs form limbs or limb-like structures whose morphogenesis depends on the characteristics of the recombination performed, particularly of the mesoderm. This experimental situation was originally devised to analyze the interactions between the ectodermal and mesodermal components of the limb bud (Zwillinget al., 1956) and permitted the identification of the specific roles played by the ectoderm and mesoderm in patterning the limb bud (MacCabe et al., 1973). More recently it has also proved useful at the molecular level for studies of gene regulation and patterning (A. Hardy et al., 1995) (Wada et al., 1998).

The fact that this experimental system permits multiple variations in the type and conditions of the components makes it an excellent system for a variety of analyses (Fernandez-Teran et al., 1999). Depending on the biological question under study, the mesoderm can be selected according to the criteria of interest including spatial and temporal origin (particular limb regions or stages), limb type (wing or leg), and degree of dissociation (single cell versus non-dissociation).

Classical work performed by John Fallon's group showed that the presence of cells of the ZPA scattered inside the RL impaired its morphogenesis. Therefore, and although the reasons underlying this observations remain elusive, the RLs have mostly been performed only with mesoderm from the anterior two thirds of the limb bud (thereafter referred to as anterior mesoderm). RLs performed with stage 20HH anterior wing mesoderm, (aRLs), form limb-like structures in which the distal segment, the autopod, and exhibits a variable number of well-formed digits of unidentifiable identity. At proximal level, a single cartilage element corresponding to the humerus, is usually identified. In the majority of cases an intermediate segment, containing a short and broad element corresponding to the radius and ulna, is also observed. The morphology of the autopod is consistently better than that of the proximal elements that is less well formed. We have suggested that the final number of digits depends on the initial size of the RL with bigger aggregates giving rise to outgrowths with more number of digits. When a fragment of ZPA or a Shh-bead is inserted into one of the margins of the RL before grafting, the limb that forms shows almost normal wing morphology particularly at distal level (Ros et al., 1994) (Fernandez-Teran et al., 1999) (**Fig.6**).

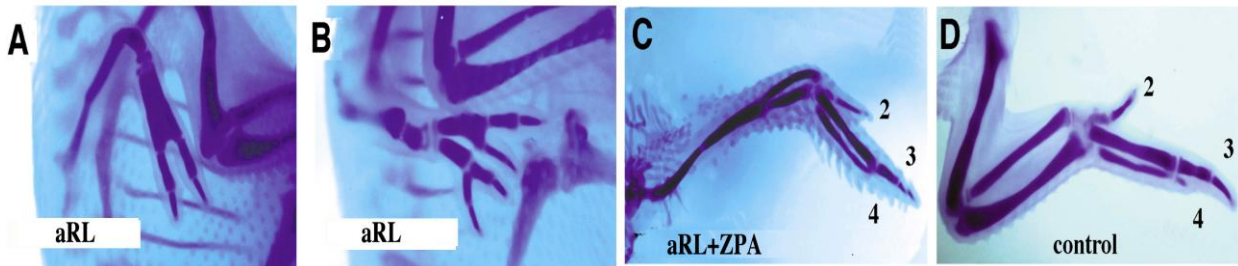


Figure 6: Limb morphologies obtained from different types of recombinant limbs 7 days after grafting. (A) and (B) show two examples of limb-like structures formed from aRL one showing two digits and the other showing 4 digits. This difference relies on the initial size of the recombinant (C) limb formed from an aRL that received a ZPA graft before grafting. Note the perfect development of the distal segment. (D) Normal wing shown for comparison.

In summary, the RL is a very powerful experimental system that has produced important insights for our understanding of the mechanisms controlling patterning in the limb bud. Recently this approach has been successfully used in molecular studies to reevaluate proximo-distal specification. (Roselló-Díez et al.; 2011, Cooper et al; 2011).

However some aspects of the development of the RLs are not completely known. For example, in the cases when the mesoderm is dissociated and reaggreated, it is unknown whether the cells reorganize or sort-out during the early phases of the RL development.

Little is known of the cell-cell interactions underlying the dynamic morphogenic events leading to the establishment of distinct skeletal structures from a population of mesenchymal cells. The manifestation of mesenchymal condensations is undoubtedly one of the most relevant steps in the formation of the cartilage template; however, it remains unknown how individual mesenchymal cells interact at a cellular level to achieve this precise three-dimensional organization. Interestingly, time-lapse experiments revealed that labeled progenitor cells rapidly sorted into distinct cellular aggregates according to their proximo-distal origin. This sorting out is achieved through the coordinated movement of individual cells (Barna and Niswander, 2007). Already within 1hr of culture, distinct proximal and distal region-specific cell aggregates formed and subsequently traveled directionally to specifically recruit additional proximal or distal cells. Subsequently, form mixed but stratified cluster in which groups of distal cells were found situated on top of proximal cells formed in these types of cultures (Barna and Niswander, 2007). Therefore, it is possible that PD sorting out also occurs in the RLs.

Thanks to the availability of GFP-transgenic chickens in our laboratory, we have decided to address this point *in vivo* and clarify whether there is some kind of sorting out in the RL system.

4. GFP-transgenic chicken

In 2004, McGrew et al., from the Roslin Institute, reported the generation of GFP-transgenic chicken (McGrew et al., 2004; 2009). They used a lentiviral vector system to produce germline transgenic birds. In these birds GFP is ubiquitously expressed and visible in both embryos and adults (**Fig.7**).



Figure 7: GFP-expressing transgenic chickens. The bird in the center is not transgenic.
(McGrew et al., 2004)

GFP-transgenic chick embryos can be used as a source for donor tissue in grafting experiments offering a unique opportunity for grafting experiments. The grafted cells can later be followed and identified by immunohistochemistry or *in situ* hybridization against GFP.

We have established a stable flock of transgenic birds at the Servicio de Estabulación y Experimentación Animal of the University of Cantabria. In this project we have used GFP-transgenic chickens to study possible cellular movements within the recombinant limb buds.

AIM OF THIS WORK

Our goal is to examine whether cells with different proximo-distal origin in the early limb bud have different properties. This would be reflected in the sorting out when intermixed in the recombinant limb situation.

To accomplish this goal we count with two excellent tools:

- a) The experimental model of Recombinant Limbs developed in the chick.
- b) The strain of transgenic GFP-expressing chicken.

For this purpose we will perform Recombinant limbs in which cells with different PD values will be marked by the *gfp* expression. The analysis of the behavior and distribution of the *Gfp*-expressing cells will allow identifying different cell properties between the cells.

Our work would produce two important results:

- a) Determine the possible existence of different cell-surface properties of distal versus proximal cells at early developmental stages in RLs.
- b) Determine the way in which the RL system should be used for patterning events.

MATERIALS AND METHODS

1. Chicken embryos

Wild type embryos: Fertilized hen eggs were obtained from local farms while *Gfp*-expressing eggs were from our farm. Both were routinely incubated at 38.5°C and 95% relative humidity. They were opened on the third day of incubation as described in Ros et al., 2000 and staged *in ovo* according to Hamburger and Hamilton (1951). The eggs were returned to the incubator until the embryo reached the desired stage.

2. Procedure to perform recombinant limbs

The recombinant limb is a limb bud-like structure created by assembling limb bud mesoderm inside a limb bud ectodermal jacket. This procedure was first devised by Zwillig who used it to study multiple processes during limb development. The procedure used here to make the RLs was based on protocols already described with some modifications (**Fig.8**; Ros et al., 2000). The ZPA was excluded from the mesoderm used to perform the recombinant limbs (anterior RLs) because this group of cells has been shown to be detrimental for the further development of the RL.

Briefly, the procedure followed to perform the RLs was:

1. Collect stage 20HH GFP and WT wing buds in separate plates with cold PBS. Dissect under the scope the regions of the limb bud needed for the particular experiment. In some cases a reticular is needed to define or measure the regions.
2. Collect limb buds from stage 22HHWT embryos.
3. Observe the collected regions (proximal and distal) under the dissecting scope to confirm that the dissection was correctly performed.
4. Digest the limb fragments in 0.5 % Trypsin in regular PBS for 9 min. at RT.
5. Incubate the whole limb buds in 0.5 % Trypsin in PBS on ice, until the pellet is ready (between 1.5 and 2h)
6. Transfer the fragments to PBS + 10% horse serum previously cold and keep them on ice for 10 min. Peel off the ectoderm.
7. Transfer the fragments to a new plate with cold PBS. Combine GFP and WT fragments as desired.
8. Wash the mesoderm fragments in PBS for 10 min. If the fragments are big cut them into halves to facilitate dissociation.
9. Transfer the mesodermal fragments to an eppendorf containing 1ml saline G+10 % Horse serum at room temperature.

10. Pipette up and down several times (8-10 times does not harm the cells) with the blue pipette tips and the pipette set up at 0.5 ml.
11. Spin down to form the pellet at 500 g for 7-10 min.
12. Incubate the tube with the pellet for half hour at 37 C
13. Detach the pellet from the bottom of the tube. Poor off in a small petri dish with Saline G + Horse serum (RT).
14. Take one limb bud from the trypsin solution transfer to ice-cold PBS+10%HS, and then to the plate with the pellet.
15. Peel off the ectoderm. Take a fragment of the pellet and stuff it into the ectoderm.
16. Repeat this step to perform as many recombinant limbs as possible/desired
17. Allow the recombinants limbs to assemble for 15 min. to 1 hour at RT.
18. To an embryo stage 20-22 HH add 2 drops of antibiotic solution. Open the membranes. Make a wound with the tungsten needle in the somites removing the ectoderm and slightly damaging the mesoderm. Transfer with a pipette one recombinant limb and position it on top of the somite's wound. Return to the incubator after 30 min.

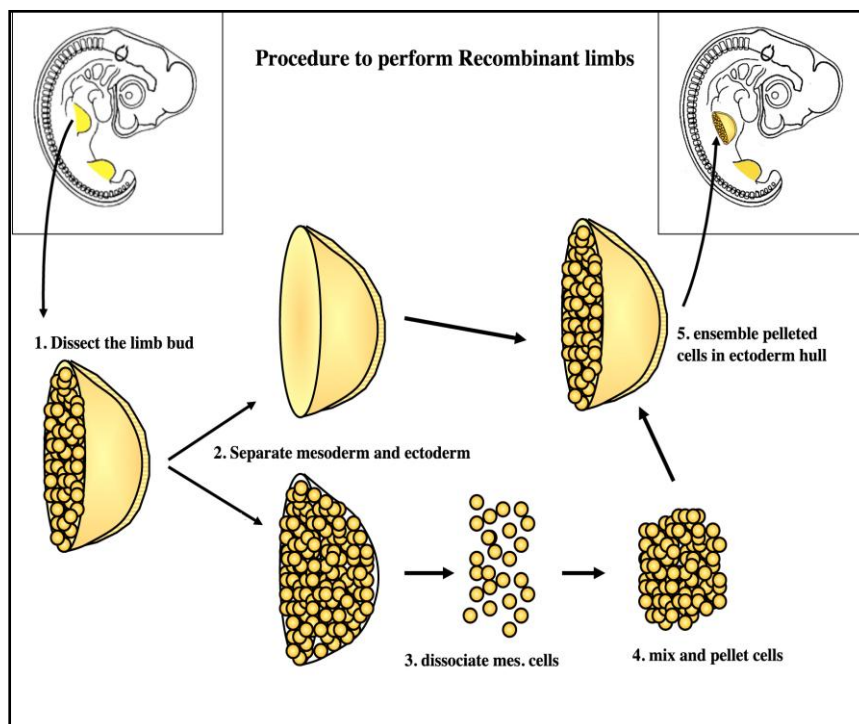


Figure 8: Drawings illustrate the procedure to perform RLs with dissociation of the limb mesoderm (Ros et al.,2000)

For our purposes we performed the following types of RLs: (Fig.9)

1. GFP Proximal + WT Distal that will be referred to as **GPWDRLs**
2. GFP Distal + WT Proximal = **GDWP**
3. Proximal GFP + WT anterior mesoderm from the complete PD axis = **GPWC**
4. Distal GFP + WT anterior mesoderm from the Complete PD axis = **GDWC**
5. GFP anterior mesoderm from the Complete PD axis and WT anterior mesoderm from the Complete PD axis = **GCWC**

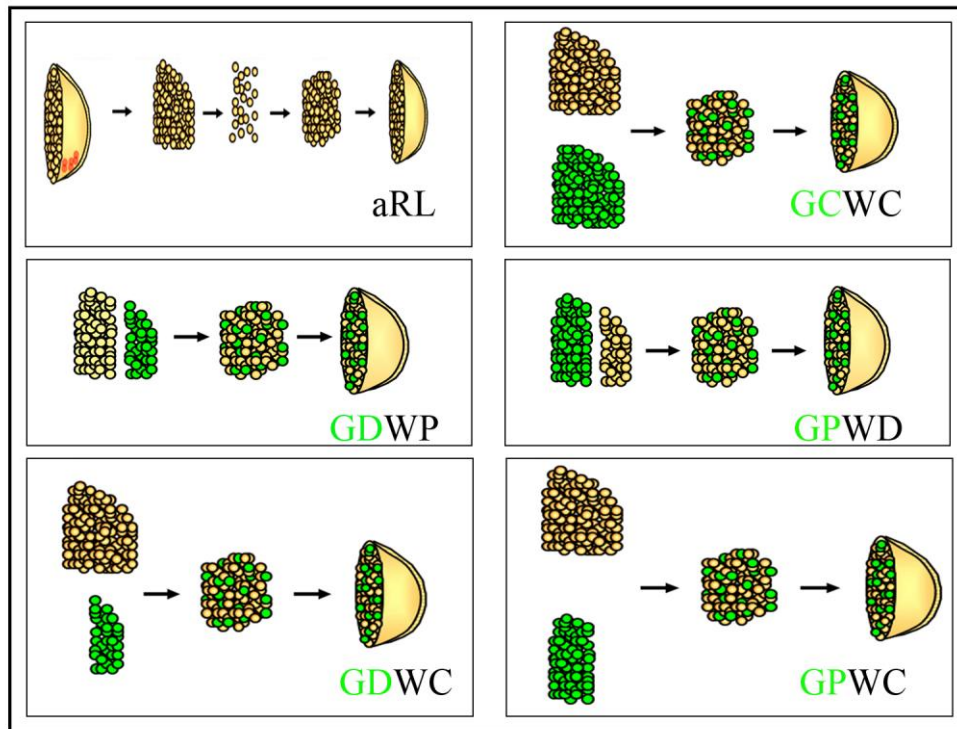


Figure 9: Drawings illustrate the different RLs performed.

3. Paraffin embedding

Paraffin embedding was performed following standard protocols. After fixation in 4% PFA, the embryos were rinsed in PBS twice and the limbs dissected out. The samples were progressively dehydrated by 10 minutes washes in rising ethanol concentrations. The samples were cleared in two changes of Xilol (10 min. each) and finally transferred to paraffin at 60°C Paraffin blocks were made with the samples in the desired orientation. A Leica RM2125RT microtome was used to obtain 7 μ m-sections which were distributed in a consecutive order in four different slides. Control limbs were processed in parallel with the RLs for comparison.

4. Whole mount *in situ* hybridization

Chick embryos were dissected in PBS and fixed in PFA 4% in PBS overnight (O/N). Next day, after washing in PBS and PBT, the embryos were dehydrated in increasing concentrations of methanol diluted in PBT and finally were stored in methanol at -20°C until needed. Before hybridization the embryos were rehydrated to PBT and bleach in H₂O₂ in PBT for 1h. After washing in PBT, they were digested in proteinase K (PK) (Roche) 10 µg/mL for a variable time depending on the stage and postfixed in 4% PFA + 0.2% glutaraldehyde. Prehybridization was performed in hybridization mixture at 65°C O/N.

Next day, the hybridization mixture was replaced by a new mixture containing the Dig-labelled antisense RNA probe and incubated O/N at 65°C. Posthybridization washes were performed at 65°C with 2% SSC-0.1% CHAPS (3x, 30 min. each) and 0.2% SSC-0.1% CHAPS (3x, 70 min, in total). Then two washes in KTBT were performed. After that, the embryos were blocked for 2-3 h at room temperature (RT) in 20% sheep serum in KTBT. In this same solution anti-dig-AP antibody (anti-digoxigenin-alkaline phosphatase antibody) was diluted 1/2000 and kept O/N at 4°C.

The following day washes with KTBT were performed at RT. Finally, alkaline phosphatase activity was detected by incubating the embryos in NTM solution with NBT (3µg/mL); BCIP (2.3µg/mL). Once obtained the desired level of signal, the reaction was stopped with several washes in KTBT and then fixed in 4%PFA.

The probe used was HoxA13.

5. *In situ* hybridization in paraffin sections

We analyzed the expression of different genes implicated in limb patterning to recombinant limbs in absence of the ZPA. Using the technique of *in situ* hybridization can demonstrate the expression of the genes that we want. In this research we used the GFP, Hox A13, Hox D13, HoxD11 and Wnt7a probes.

To perform the ISH over our paraffin sections, previously, we dewaxed them by immersion in to Xilol and then rehydrated them in decreasing ethanol washes.

We put in PBT before digestion with proteinase K for 7 minutes and 30 seconds. We washed in PBS and fix in 4% paraformaldehyde. We treated with acetic anhydride. The sections were incubated overnight in hybridization mixture containing the desired antisense RNA labeled with digoxigenin. After posthybridization, washes in SSC and MABT were performed, and the sections were blocked and incubated overnight with the antibody α-DIG-AP (1:2500). Next day the signal was revealed by NTM/NBT/BCIP.

Finally the sections were fixed in 4% PFA and mounted with Cytoseal.

RESULTS

1. Cells with different proximo-distal origin sorting out in the Recombinant Limb situation and localize according to their origin

To examine possible sorting out of proximal and distal cells, we performed RLs with anterior limb bud mesoderm but with either proximal or distal mesoderm obtained from GFP-expressing chicken embryos (see Material and Methods). The proximo-distal extension of the 20HH limb bud is about 500microns. After discarding the posterior mesoderm that includes the ZPA, the mesoderm was divided into proximal and distal regions of about 250 microns each by sectioning along the AP axis of the limb bud. After removal of the ectoderm, proximal stripes of WT embryos were mixed with distal stripes of GFP-transgenic embryos and dissociated to single cell level and reaggregated to make **GDWP** (Green distal/wild type proximal) RLs. We also performed RLs with the complementary mixture of cells: proximal GFP-cells were mixed with distal WT cells that we termed **GPWD** (Green proximal/wild type distal). For these two types of RLs the proportion of *Gfp*-marked cells to WT-cells was 1:3. A scheme showing the mesodermal component in these two types of RLs is shown in **Fig.9** (see Material and Methods).

Expression of *Gfp* was used to mark the *Gfp*-expressing cells. Several methods were evaluated including the direct analysis of the endogenous fluorescence and immunohistochemistry or ISH for *Gfp*. We found that the endogenous fluorescence was not appropriate for our study because the fixation and embedding procedure highly attenuated the fluorescence. We decided to use ISH because of the clean results obtained. These pilot experiments also indicated that the position of the *Gfp*-expressing cells was much easier to appreciate when the amount of marked cells was reduced relative to the amount of unmarked cells. For this reason, we performed the RL with 3 times less marked cells than unmarked cells.

There is evidence that proximal and distal cells can be distinguished as early as stage 19HH by their sorting behavior in vitro (Barna and Niswander, 2007). Therefore, we predicted that if this behavior also occurred in the RL situation, the marked cells will be found predominantly in the proximal or distal region of the recombinant, as corresponded to their origin.

24h after grafting, the RL formed a limb bud emerging from the back of the embryo between the normal wing and leg. The AER was always clearly observed (arrowheads in **Fig.10A**). The ISH for *Gfp* nicely marked the *Gfp*-expressing cells that in the **GDWP** RL were observed all along the PD axis of the recombinant limb (**Fig. 10A**) but much more abundant in the distal region. Interestingly, in the **GPWDRL**, the *Gfp*-expressing cells were abundantly distributed throughout the PD axis of the RL

except in the distal area, just under the AER, and in the stripe of mesoderm subjacent to the ectoderm where they were very scarce (**Fig. 10B**).

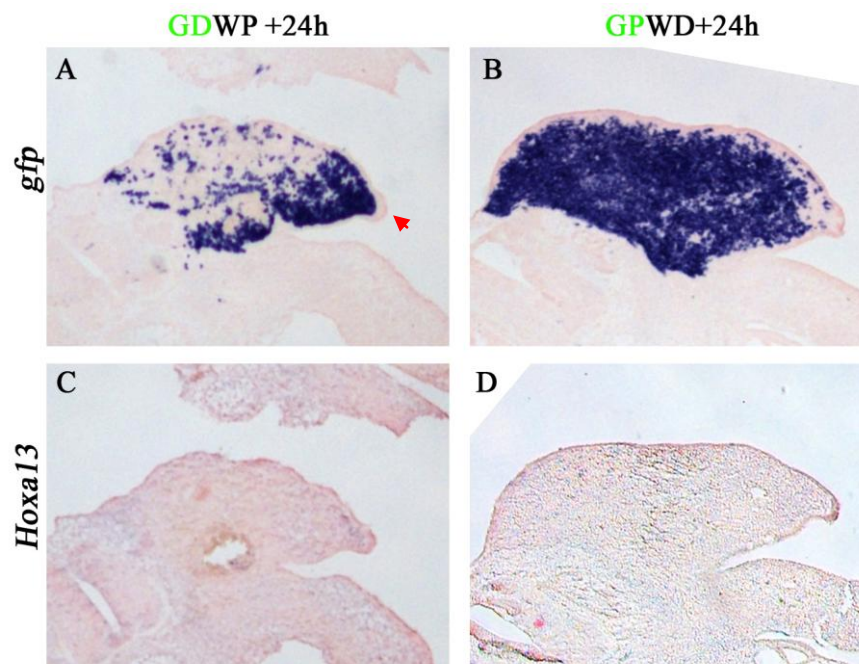


Figure 10: Expression patterns of *Gfp* and *Hoxa13* genes in RLs. The type of RL is indicated at the top and the probe used for the ISH on the left. (**A**) and (**C**) are consecutive longitudinal sections of the same GDWP RL hybridized 24 h after grafting with *Gfp* and *Hoxa13* probes respectively. Note that *Gfp*-expressing cells form clusters and that they predominantly localize at distal level. (**B**) and (**D**) are consecutive longitudinal sections of the same GPWD RL hybridized 24h after grafting with *Gfp* and *Hoxa13* probes respectively. Note that *Gfp*-expressing cells are abundant all along the RL except in a small stripe of mesoderm under the AER and under the dorsal and ventral ectoderm. The activation of *Hoxa 13* is barely detectable under the AER in (**C**) while it has not yet started in (**D**) at this stage.

Concomitantly with the analysis of the distribution pattern of *Gfp*-expressing and non-expressing cells we also analyzed how patterning along the proximo-distal axis was specified in the RL. For this we decided to analyze the expression of *Hoxa13*, a marker of the autopod that is activated by stage 22HH in a small posterior-distal area of the wing bud (**Fig. 11**). *Hoxa13* is not expressed at the time the mesoderm is collected to perform the RLs.

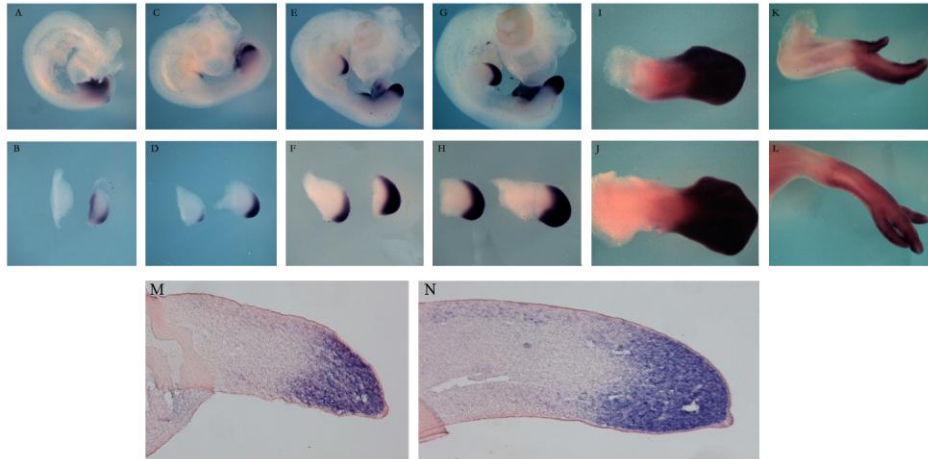


Figure 11: Pattern of *Hoxa13* expression in chick embryos. Whole mount *in situ* hybridization to show the evolution of *Hoxa13* pattern of expression during limb development. (A) Chick stage 21HH. (B) Wing and leg of the embryo in A. (C) Chick stage 23HH. (D) Wing and leg of the embryo in C. (E) Chick stage 24HH. (F) Wing and leg of the embryo in E. (G) Chick stage 25HH. (H) Wind and leg of the embryo in G. (I) and (J) show the wing and leg of a stage 30HH chick embryo. (K) and (L) show the wing and leg of a stage 35HH chick embryo. (M) and (N) show the expression of *Hoxa13* after *in situ* hybridization in paraffin sections in control limbs.

24 hours after grafting, expression of *Hoxa13* was undetectable in the majority of specimens. This is an expected result as the developmental age of the RL corresponds to about stage 22HH (Fig.11) when normal expression is starting to be activated and it fits with previously published results showing that activation of *Hoxa13* occurs in the distal cells of the RLs between 24 and 30 hours after grafting (Piedra et al. 2000). Accordingly, *Hoxa13* transcripts were detected under the AER of some specimens (Fig.10C), indicating correspondence with the normal time of activation.

48 hours after grafting the RLs have notably increased size indicating their appropriate development (Fig. 12). At this time point the distribution of *Gfp*-expressing cells both in **GDWP** and **GPWD** RLs follows the same pattern described in the specimens collected 24 hours after grafting. This is, cells of distal origin were predominantly found distally although some clusters of cells are found all along the PD axis. Cell with proximal origin are less abundant at distal origin. There is a clear trend towards cells been localized in the region from which they were originally obtained. At this stage, the expression of *Hoxa13* has been activated and a distal domain of expression, similar to normal embryos of similar stage (Fig. 12C-D), has been clearly established.

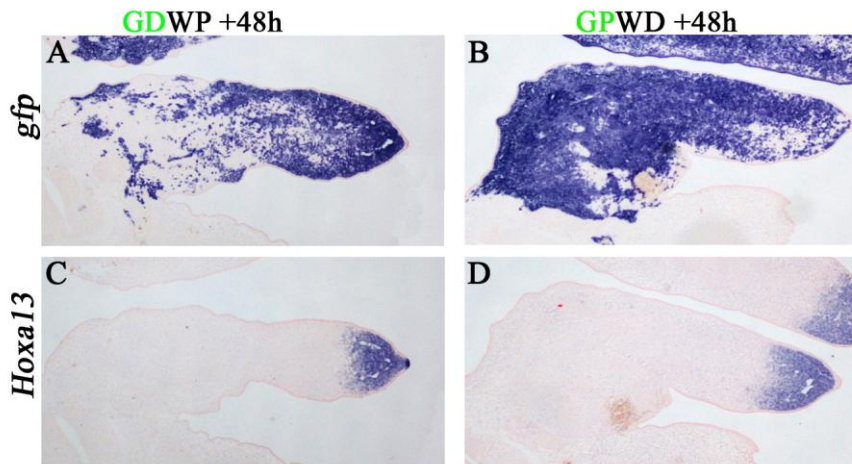


Figure 12: Expression patterns of *Gfp* and *Hoxa13* genes in RL. (A) and (C) are consecutive longitudinal sections of the same GDWPRL hybridized 48 h after grafting with *Gfp* and *Hoxa13* probes respectively. *Gfp* expression is observed all along the PD axis of the RL but the presence of *Gfp*-expressing cells is most conspicuous at distal level. (B) and (D) are consecutive longitudinal sections of the same GPWDRL hybridized 24 h after grafting with *Gfp* and *Hoxa13* probes respectively. The proximal *Gfp*-expressing cells are found all along the RL but they are much less abundant under the AER. Note that at this stage *Hoxa13* has been activated in the distal mesoderm in both types of RLs.

Together these results indicate that cells with similar PD origin cluster together and segregate from cells with different PD origin. Furthermore, there is a tendency for cells to localize according to their origin suggesting active movements of cluster of cells. This tendency seem to be sharper for distal than for proximal cells. Finally, this cell reorganization occurs during the first 24 hours of development of the RL and it is subsequently maintained.

Interestingly, some bias toward the dorsal or ventral side of the RLs was also observed in the distribution of the *Gfp*-expressing cells. Dorso-ventral patterning in the limb bud is controlled by the non-AER ectoderm that expresses *Wnt7a* dorsally and *Engrailed1* ventrally. It should be noted that when performing the RLs we did not keep track of the dorso-ventral axis of the ectodermal hull and therefore it is not known whether it matches or not with the dorso-ventral axis of the embryo. The expression of *Wnt7a* was analyzed in the RLs (not shown) but we were unable to detect any preference of distal cells towards the dorsal ectoderm but rather a preference towards the ectoderm.

The expression of *Hoxa13* confirms the normal development of the RL as it has been already published that its activation occurs between 24 and 30 hours after grafting (Piedra et al. 2000). The expression of *Hoxa13* in its correct domain also indicates that the specification of the autopod occurs according to the position of the cells in the RL and not to their origin.

Finally, another observation from our experiments is that the marked cells appear to be more abundant than the unmarked cells, even though marked cells were 3-fold times less numerous than unmarked cells in the pellet. This is very likely due to the amplification of the staining method used but prompted us to further reduce the number of marked cells in subsequent experiments.

2. The distribution of cells correlates with their Proximo-distal origin

We next decided to explore the possible PD sorting-out of limb mesenchymal cells in a different situation. We mixed distal *Gfp*-expressing cells or proximal *Gfp*-expressing cells with WT limb mesoderm from the complete PD axis. We performed two types of combinations: **GDWC** (Green distal wild type complete) and **GPWC** (Green proximal wild type complete) respectively (**Fig.13**). Since in this case there are both proximal and distal WT cells, the marked cells can intermingle with WT of similar PD origin. Our prediction was that this combination should make clusters more difficult to identify while facilitating the detection of cells as they will be diluted with WT cells. Also, as previously mentioned, to facilitate the visualization of the *Gfp*-expressing cells they were added in a reduced proportion. The proportion of marked to WT cells in this experiment was 7:1.

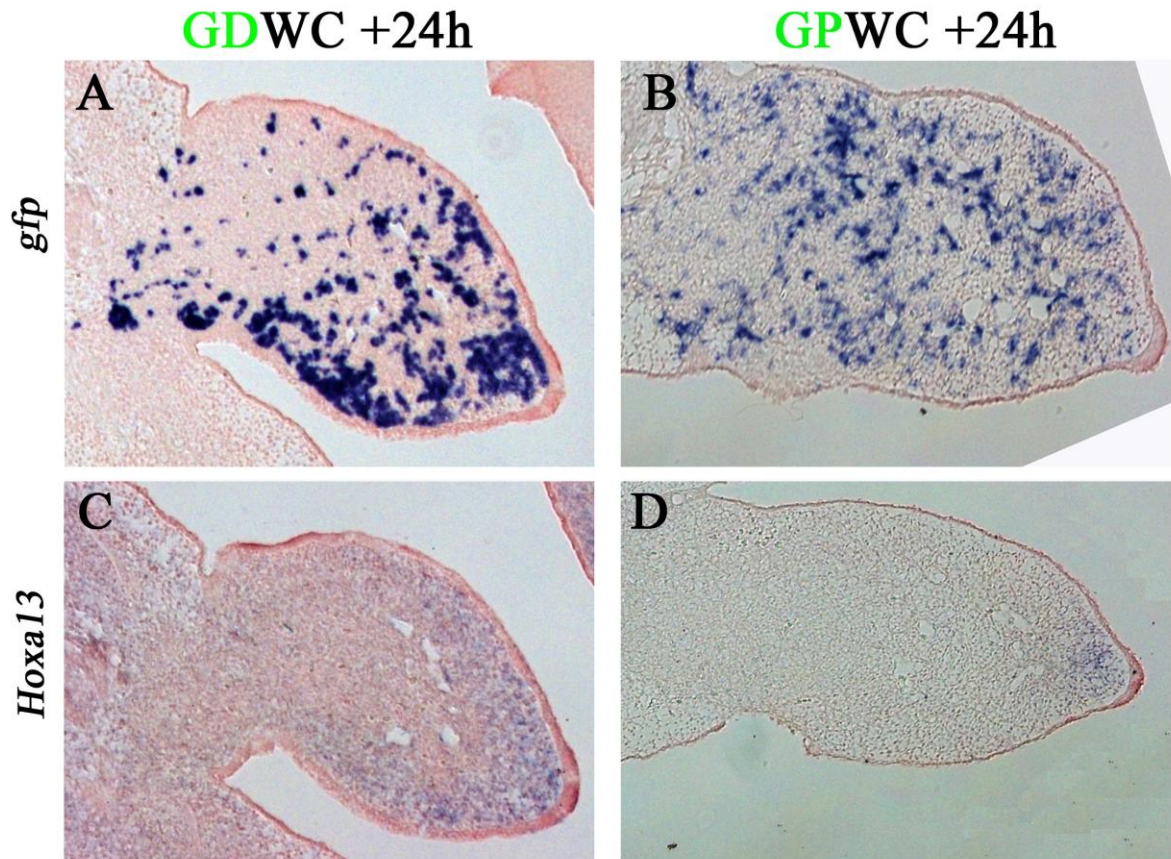


Figure 13: Expression patterns of *Gfp* and *Hoxa13* genes in RL. (A) and (C) are consecutive longitudinal sections of the same GDWC RL hybridized 24 h after grafting with *Gfp* and *Hoxa13* probes respectively. As expected, more individual *Gfp*-expressing cell share observed but their preferential localization is distal and peripheral. (B) and (D) are consecutive longitudinal sections of the same GPWC recombinant limb hybridized 24h after grafting with *Gfp* and *Hoxa13* probes respectively. Note the uniform distribution of proximal *Gfp*-expressing cells in the RL except under the AER and ectoderm. At this stage *Hoxa13* is been activated in the distal mesoderm in both types of RLs.

24 hours after grafting, the distal *Gfp*-expressing cells were found all along the PD axis of the RL but clearly more abundant distally and in the periphery. This observation further points to a differential behavior of proximal versus distal cells and supports a shorting out of distal and proximal cells. Also, the reciprocal type of cell mixing, proximal *Gfp*-expressing cells with WT cells from the complete PD bud, leads to a very homogenous distribution of the proximal cells inside the recombinant except in a band subjacent to the AER and ectoderm where they are scantily found (Fig.13).

When comparing Fig.13A and Fig.13B, it is possible to appreciate that there are no clear cell clusters in the GPWC RL. There was one difference between the procedures followed to perform the

two types of RL in **Fig.13**. This is that the dissociation procedure was more intense to perform the **GPWC** pellet. We increased the number and intensity of pipetting to assure that the dissociation was to single cell level because there are evidences that the association of a few cells favors the formation of clusters (Barna and Niswander, 2007). As shown in **Fig.14**, clusters of 3-4 cells could be appreciated in the pellet used for the **GDWC** (**Fig. 14A** shows the pellet used for RL in **Fig. 13A**) while there were not in the pellet used for the **GCWC** (**Fig. 14B** shows the pellet used for RL in **Fig. 16**). This result indicates that the initial existence of cluster of cells favors the subsequent formation of bigger cell aggregates.

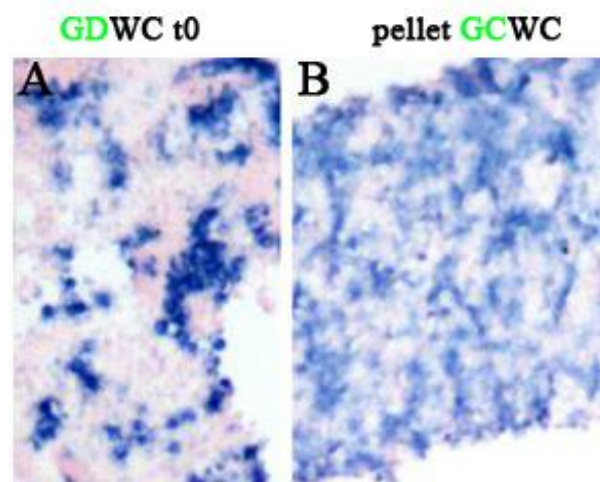


Figure 14: Expression pattern of *Gfp* in the cell pellets used to perform the RL shown in Fig. 13 and Fig.16. (A) GDWC RLs at time 0. (B) Pellet of GCWC before performing the RL. Note in (A) the presence of some cluster of cells while in (B) there is a homogeneous distribution of green and wild type cells.

As expected, *Hoxa13* expression is activated and progresses in the RL in the normal pattern disregarding the origin and mixing of the mesodermal cells (**Fig.15**).

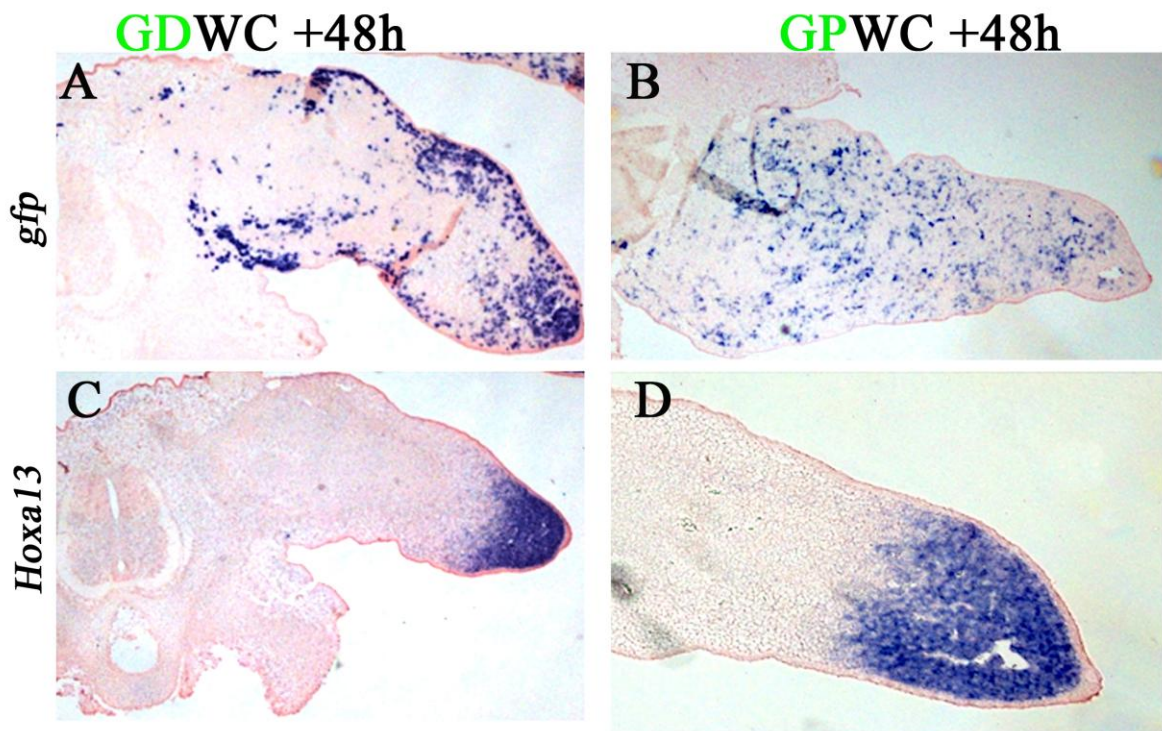


Figure 15: Expression patterns of *Gfp* and *Hoxa13* genes in RL. The type of RL is indicated at the top of the Figure and the probe use on the left. (A) and (C) are consecutive longitudinal sections of the same **GDWC** RL 48h after grafting. *Gfp*-expressing cells are observed all along the PD axis of the RL but most conspicuous at distal and peripheral levels. (B) and (D) are consecutive longitudinal sections of the same **GPWC** recombinant limb 48h after grafting. Note that the pattern of distribution of distal and proximal cells observed 24h after grafting is maintained. At this stage *Hoxa13* occurs in the distal mesoderm in both types of RLs similar to WT limb buds.

3. The expression of *Gfp* is not the cause of the sorting out between proximal and distal cells

It is possible that in the previous experiments the expression of *Gfp* may influence the behavior of the cells. To check this, we performed RL mixing anterior mesoderm cells of the complete PD axis from both WT and *Gfp*-expressing cells.

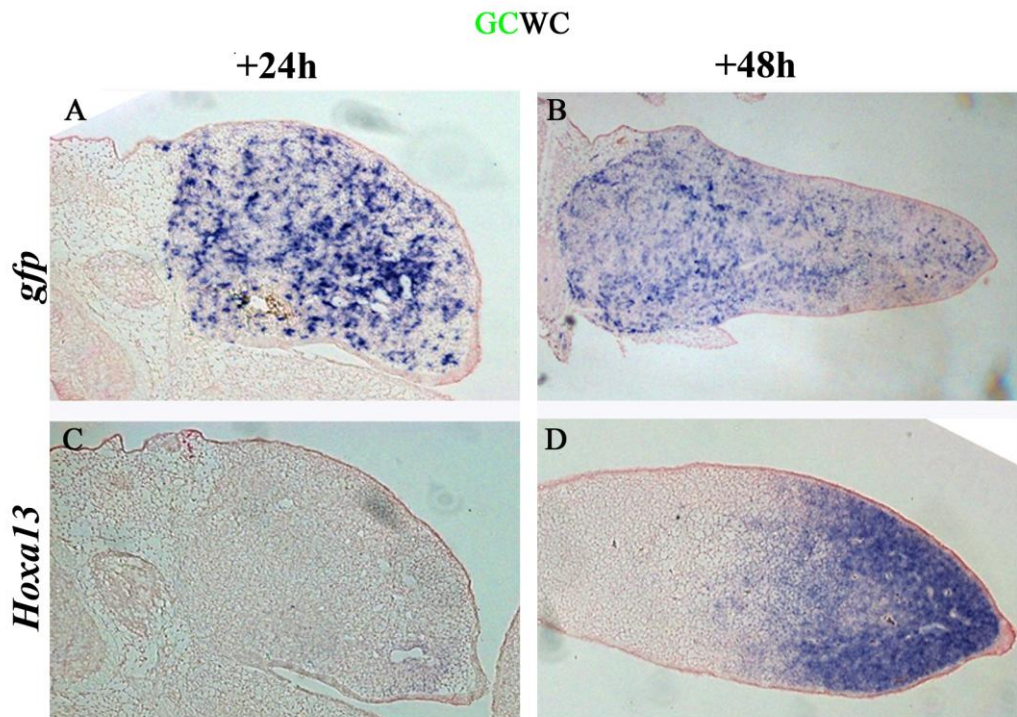


Figure 16: Expression pattern of *Gfp* and *Hoxa13* genes in GCWC RLs. (A) and (C) are consecutive longitudinal sections of the same GCWC RL hybridized 24 h after grafting with *Gfp* and *Hoxa13* probes respectively. *Gfp*-expressing cells are observed uniformly distributed all along the RL. (B) and (D) are consecutive longitudinal sections of another GCWC recombinant limb hybridized 48 h after grafting with *Gfp* and *Hoxa13* probes respectively. Note the uniform distribution of *Gfp*-expressing cells in the RL. At this stage *Hoxa13* has been activated in the distal mesoderm (D).

When analyzing the distribution of the cells, we observe uniform distribution of distal and proximal cells along the PD axis of the RL fixed 24h after grafting (**Fig.16A**) and 48h after grafting (**Fig.16B**) indicating that the expression of *Gfp* has no effect *per se* in the sorting out of the cells.

As expected, *Hoxa13* show normal expression in both RLs (**Fig.16 C, D**).

DISCUSSION

In this work we have generated RLs in which the PD origin of individual cells can be tracked thanks to the use of transgenic chicken that ubiquitously express *Gfp*. This procedure has allowed us to assess possible differential behaviors in early limb bud cells with different proximal and distal origin.

We have performed RLs with anterior mesoderm from stage 20HH limb buds. The limb bud mesoderm was divided into proximal and distal regions and, depending on the type of RL performed, proximal or distal stripes were obtained from *Gfp*-expressing chicken. The distribution of *Gfp*-expressing cells during the subsequent development of the RL was analyzed by ISH. Our study yields two important results:

- a) Early limb bud mesodermal cells segregate according to their PD origin.
- b) The distribution of the cellular aggregates correlates with their PD origin.

The sorting-out between limb bud mesenchymal cells has been previously widely explored but mainly in culture and between cells of different developmental stages (Wada et al., 1994; Ide et al., 1994; Omi et al., 2002). However, it has also been shown that proximal and distal cells display distinct cellular properties from very early stages of limb bud development (19HH) and that they sort out in vitro (Barna and Niswander, 2007). Here we show a similar cell sorting behavior in the RL situation reflecting unique cell properties of proximal and distal cells at stage 20HH. This sorting out behavior needs to be taken into consideration in the future for the correct interpretation of the morphogenetic ability of RLs as it can influence pattern formation.

It work mentioning that the cell aggregates seem to be larger when the initial dissociation is not complete and some clusters of 2-4 cells remain. This is supported by the observation that within one hour of culture distinct proximal or distal small cell aggregates form that subsequently move to recruit more proximal or distal cells (Barna and Niswander, 2007). It is possible that the initial level of dissociation favors the formation of bigger aggregates facilitating the sorting out and redistribution of cells.

Our results also show that the clusters of proximal and distal cells can travel considerable distances. This is particularly true for distal cells that are mainly found under the AER 24h after grafting whereas they were uniformly distributed initially. Interestingly, in the RL we observe a complementary redistribution of proximal and distal cells. While distal cell locate under the ectoderm, mainly under the AER, proximal cells are predominantly excluded from these regions. This indicates that the ectoderm provides signals that influence the dynamic movements of the cells and that these signals have opposite effect on proximal versus distal cells. Fgfs are likely candidates as it has been

shown that they maintain a high level of mobility in distal cells (Gross et al., 1996). It is also possible that proximal signals from the embryonic flank may influence the behavior of the cells attracting proximal cells while repelling distal cells. A possible candidate for the proximal signal is RA although this is highly controversial at present (Roselo-Diez et al., 2011; Cunnigahm et al., 2013).

Sorting out and redistribution of cells occur very fast after the RL is assembled. In this work, we have first analyzed 20 hours after grafting and the new situation had already been established. A time course analysis will be needed in the future to more precisely understand the temporal dynamics of the cell segregation and cell movements.

Although we have not explored the molecular basis for the sorting out and redistribution, based on previous studies it seems reasonable to assume that it relays on differential cell adhesion properties between proximal and distal cells. It is known that during limb bud development cell adhesion molecules are expressed in a spatio-temporal specific manner and Ephrin-Eph interactions and cadherins are good candidates (reviewed in Wada et al., 2011).

The RL is a powerful experimental approach that has provided important insights for our current understating of how limb patterning is generated. This is a very versatile system that permits many variations one of which implies the dissociation of the limb bud mesoderm. The limb bud mesoderm is dissociated to single cell level, compacted by mild centrifugation and repacked into an ectodermal hull. In this new situation the cells lose their original positional information and, under the influence of ectodermal signaling, acquire new positional information. Our results reveal that, despite the single cell dissociation and the randomly reaggregation, the cells in the RL rapidly sort out and redistribute according to their original PD positional information. Therefore, these rapid reorganization movements inside the RL need to be taken into account in the future for a correct interpretation of the morphogenetic capacity of limb bud cells.

CONCLUSIONS

1. *Gfp*-expressing cells are easily tracked in the RL situation.
2. In the RL situation, cells sort out according to their PD origin.
3. In the RL situation, cells are preferentially found in the position corresponding to their
4. The re-distribution of distal cells indicates active cell movements that occur very rapidly after the formation of the RL. They may respond to a positive signal from the AER (Fgfs) or to a negative signal from the flank (Retinoic acid).
5. It is possible that the level of initial dissociation may influence the subsequent formation of cell aggregates.
6. Disregarding sorting-out and reorganizing movements, PD patterning is normally established in the RL, accordingly to the expression of the autopod marker gene *Hoxa13*.

FUTURE EXPERIMENTS

At first, we want to repeat the all experiments but pippeting more intense to dissociating in a single cells levels to see if the cells sort out or not.

Although we don't referee in this project, we did experiments with a new slide provided by IBIDI Company. The microfluidic channel of the μ -Slide is suited to set up chemical gradients. By a simple pipetting procedure a concentration profile can be established. Our goal is growing mesodermal cells into the channel and apply our chemoattractant in one reservoir (Fgfs or Retinoic acid) to analyze by immunoflourescence the sorting out or not sorting out of the cells. Is expected that if we add Fgfs proteins in one reservoir, distal cells move to this point.

ACKNOWLEDGEMENTS

I am grateful to Marian Ros, director of this project, for her help and support during the preparation of this work. I also thank M^a Félix and Patricia Saiz for critical reading of this thesis and Marisa Junco, Endika Haro and Carlos Garrido-Allepuz for their ideas and their help every day.

I am thankful to Lucia Carrera, Paula Ruiz and Ana Mateos for making me stay nice both inside and outside the laboratory.

In general, I am very grateful to all the members of Ros's Lab because they have always helped and we have passed nice moments working together.

This work has been supported by the Spanish Government (grant BFU2011-24972 to M.A.R.).

REFERENCES

- Altabef, M., Tckle, C., 2002. Initiation of dorso-ventral axis during chick limb development. *Mech. Dev.* 116, 19-27.
- Ahn, D.G., Kourakis, M.J., Rohde, L.A., Silver, L.M., Ho, R.K., 2002. T-box gene *tbx5* is essential for formation of the pectoral limb bud. *Nature.* 417, 754-8.
- Barna, M., Niswander, L., 2007. Visualization of cartilage formation: Insight into cellular properties of skeletal progenitors and chondrodysplasia syndromes. *Developmental cell.* 12, 931-941.
- Bastida, M.F., Delgado, D., Wang, B., Fallon, J.F., Fernández-Terán, M., Ros, M.A., 2004. Levels of Gli3 repressor correlate with *bmp4* expression and apoptosis during limb development. *Developmental dynamics* 231: 148-160.
- Bastida, M.F., Shet, R., Ros, M.A., 2009. A BMP-Shh negative feedback loop restricts Shh expression during limb development. *Development.* 136, 3779-89.
- Bénazet J.D., Zeller, R., 2009. Vertebrate limb development: Moving from classical morphogen gradients to an integrated 4-dimensional patterning system. *Cold Spring Harbor Perspectives in Biology* 1:a001339.
- Butterfield, N.C., McGlenn, E., Wicking, C., 2010. The molecular regulation of vertebrate limb patterning. *Developmental Biology.* Vol.90.0070-2153.
- Cunningham, T.J., Zhao, X., Sandell, L.L., Evans, S.M., Trainor, P.A., Duester, G., 2013. Antagonism between retinoic acid and fibroblast growth factor signaling during limb development. *Cell reports* 3, 1-10.
- Davis, A.P., Holmyard, D.P., Millen, K.J., Joyner, A.L. 1991. Examining pattern formation in mouse, chicken and frog embryos with an En-specific antiserum. *Development.* 111, 287-98.
- Dealy, C.N., Roth, A., Ferrari, D., Brown, A.M., Kosher, R.A., 1993. Wnt-5a and Wnt-7a are expressed in the developing chick limb bud in a manner suggesting roles in pattern formation along the proximodistal and dorsoventral axes. *MEch. Dev.* 43, 175-86.

Fernández-Terán, M., Piedra, E., Ros, M.A., Fallon, J.F., 1999. The recombinant limb as a model for the study of limb patterning, and its application to muscle development. *Cell Tissue Res* 296: 121-129.

Gardner, C.A., Barald, K.F., 1992. Expression patterns of engrailed-like proteins in the chick embryo. *Dev Dyn.* 193, 370-88.

Laufer, E., Nelson, C.E., Johnson, R.L. Morgan, B.A., Tabin, C., 1994. Sonic hedgehog and Fgf-4 act through a signaling cascade and feedback loop to integrate growth and patterning of the developing limb bud. *Cell.* 79, 993-1003.

Mariani, F.V., Ahn, C.P., Martin, G.R., 2008. Genetic evidence that FGFs play an instructive role in limb proximal-distal patterning. *Nature.* May 15; 401-405.

Mercader, N., Leonardo, E., Piedra, M.E., Martínez-A., C., Ros, M.A., Torres, M., 2000. Opposing RA and FGF signals control proximodistal vertebrate limb development through regulation of Meis genes. *Development* 127, 3961-3970.

Omi, M., Anderson, R., Muneoka, K., 2002. Differential cell affinity and sorting of anterior and posterior cells during outgrowth of recombinant avian limb buds. *Developmental biology* 250, 292-304.

Parr, B.A., McMahon, A.P., 1995. Dorsalizing signal Wnt-7 a required for normal polarity of D-V and A-P axes mouse limb. *Nature.* 374, 350-3.

Parr, B.A., Shea, M.J., Vassileba, G., McMahon, A.P., 1993. Mouse Wnt genes exhibit discrete domains of expression in the early embryonic CNS and limb buds. *Development.* 119, domains of expression in the early embryonic CNS and limb buds. *Development.* 119, 247-671.

Piedra, M.E., Rivero, B.F., Fernández-Terán, M., Ros, M.A., 2000. Pattern formation and regulation of gene expressions in chick recombinant limbs. *Mechanisms of Development* 90. 167-179.

Pizzete, S., Abate-Shen, C., Niswander, L., 2001. BMP controls proximodistal outgrowth, via induction of the apical ectodermal ridge, and dorsoventral patterning in the vertebrate limb. *Development.* 128, 4463-74.

Ridle, R.D., Ensini, M., Nelson, C., Tsuchida, T., Jessel, T.M., Tabin, C., 1995. Induction of the LIM homeobox genes *Lmx1* by WNT7a establishes dorsoventral pattern in the vertebrate limb. *Cell*. 83, 631-40.

Ridle, R.D., Johnson, R.L., Laufer, E., Tabin, C., 1993. Sonic hedgehog mediates the polarizing activity of the ZPA. *Cell*. 75, 1401-16.

Ros, M.A., Simandi, B.K., Clark, A.W., Fallon, J.F., AÑO??. Methods for manipulating the chick limb bud to study gene expression, tissue interactions and patterning. *Developmental biology protocols*. Vol. 137

Ros, M.A., Lyons, G.E., Mackem, S., Fallon, J.F., 1994. Recombinant limbs as a model to study homeobox gene regulation during limb development. *Developmental Biology*. 166, 59-72.

Roselló-Díez, A., Ros, M.A., Torres, M., 2011. Diffusible signals, not autonomous mechanism, determine the main proximodistal limb subdivision. *Science* 332, 1086.

Tabin, C., Wolpert, L., 2007. Rethinking the proximodistal axis of the vertebrate limb in the molecular area. *Genes Dev*. 21, 1433-42.

Vogel, A., Rodriguez, C., Warnken, W., Izpisua Belmonte, J.C., 1995. Dorsal cell fate specified by chick *Lmx1* during vertebrate limb development. *Nature*. 378, 716-20.

Wada, N., 2011. Spatiotemporal changes in cell adhesiveness during vertebrate limb morphogenesis. *Developmental dynamics* 240:969-978.

Wada, N., Uchiyama, K., Ide, H., 1993. Cell sorting and chondrogenic aggregate formation in limb bud recombinants in culture. *Development. Growth & Differentiation*., 35(4). 421-430.

Wyngaarden, L.A., Hopyan, S., 2008. Plasticity of proximal-distal cell fate in the mammalian limb bud. *Developmental Biology*. 313, 225-233.